Submission code: L7X8NYJK7V

See this and other abstracts on our website: https://home.sbgf.org.br/Pages/resumos.php

Comparison Between Acoustic and Pseudo-Acoustic VTI Modeling Applied to the Marmousi Model

Juan Marques, Felipe Costa (GISIS/UFF), Marco Cetale (GISIS/UFF)

Comparison Between Acoustic and Pseudo-Acoustic VTI Modeling Applied to the Marmousi Model

Abstract Summary

This work aims to compare the numerical modeling of seismic wave propagation using the acoustic wave equation and the pseudo-acoustic wave equation in vertically transversely isotropic (VTI) media. Initially, the numerical models were validated by comparing the numerically obtained phase velocity with the analytical solution. After validation, a main scenario was analyzed: the Marmousi model. The comparison between the seismograms generated by both methods allowed the evaluation of the residual between the responses, highlighting the differences in each wave propagation approximation.

Introduction

Numerical modeling of seismic wave propagation is widely used in geophysics, with the acoustic wave equation being an attractive choice due to its relative low computational cost. However, this approach assumes isotropy of the medium, which limits its accuracy in environments where anisotropy is significant. To overcome this limitation, VTI pseudoacoustic models are employed, as they represent anisotropic effects while maintaining computational efficiency. This work compares and analyzes the acoustic and VTI pseudoacoustic approaches applied to the anisotropic Marmousi model.

Theory

The approximation introduced by Tsvankin (1997) uses the exact phase velocity and assumes the shear wave (qSV) velocity to zero:

$$\lim_{v_{sz}\to 0} v_p^2(\theta) = v_{pz}^2 \left(1 + \epsilon \sin^2\theta - \frac{1}{2} + \frac{1}{2}\sqrt{\left(1 + 2\epsilon \sin^2\theta\right)^2 - 2(\epsilon - \delta)\sin^2 2\theta}\right). \tag{1}$$

Where v_{pz} is the P-wave velocity propagation, θ is the phase angle, ϵ and δ are Thomsen's anisotropic parameters.

The equation used to describe wave propagation in VTI media can be expressed as proposed by McGarry and Moghaddam (2009):

$$\frac{1}{v_{pz}^2}\frac{\partial^2 p}{\partial t^2} = (1 + 2\epsilon)\frac{\partial^2 p}{\partial x^2} + \frac{\partial^2 q}{\partial z^2} \tag{2}$$

$$\frac{1}{v_{pz}^2}\frac{\partial^2 q}{\partial t^2} = (1 + 2\delta)\frac{\partial^2 p}{\partial x^2} + \frac{\partial^2 q}{\partial z^2}. \tag{3}$$

Where p represents the pressure field and q is an auxiliary field.

In this work, second-order time derivatives and eighth-order spatial derivatives were used for the VTI pseudo-acoustic formulation. To avoid undesired reflections at the model boundaries we apply the absorbing boundary condition proposed by Cerjan et al. (1985). The signal used to generate the impulse source was a Ricker wavelet with a 60 Hz of cutoff frequency. For all simulations, dispersion and stability criteria are controlled using the following relations:

$$h \leq \frac{v_{\min}}{G.f_{\text{cut}}} \qquad \text{and} \qquad \Delta t \leq \frac{h}{\beta.v_{max}} \tag{4}$$

Where v_{min} is the minimum velocity of the medium, f_{cut} is the cutoff frequency of the seismic source, and G is a constant depending on the spatial derivative order. The maximum phase velocity, $v_{max} = v_{pz}\sqrt{1+2\epsilon}$, is determined by the vertical velocity v_{pz} and the Thomsen parameter ϵ. Additionally, β is a factor depending on the time discretization.

Methodology

The first test (Figures 1a and 1b) validated the numerical solution by comparing it to the analytical phase velocity (Equation 1) in a homogeneous medium with constant parameters: $v_p = 3000$ m/s, $\epsilon = 0.2$, and $\delta = 0.2$. For the validation, a seismic source was placed at the center of the model, allowing wave propagation symmetry to be observed and numerical results to be compared to the analytical phase velocity expression in VTI media.

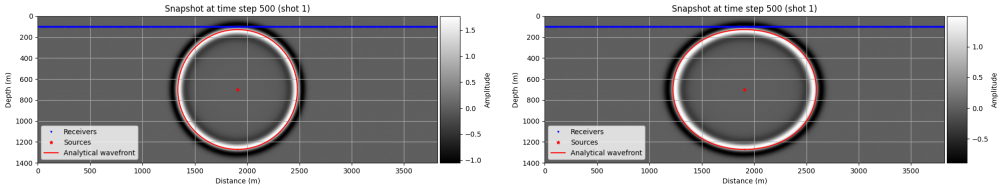

(a) (b)

Figure 1: Comparison between the numerical and analytical solutions of phase velocity in a homogeneous VTI medium with $\epsilon = \delta = 0.2$. (a) Wavefield generated by the isotropic acoustic model. (b) Wavefield generated by the pseudo-acoustic VTI model. The figures show the wavefields at time t = 0.25 s.

A notable feature was observed, as reported in the literature for the VTI pseudo-acoustic model: when ϵ and δ differ, an energy artifact appears. Figure 2a shows this artifact propagating more slowly than the P-wave in VTI media. Despite its unusual appearance, this phenomenon corresponds to the propagation of the qSV mode, even in anisotropic acoustic models. The equation derived from Alkhalifah (1998), which assumes zero shear velocity, does not eliminate this mode, as it is related to anisotropy contrasts.

Alkhalifah (1998) showed that placing the source in an isotropic region can suppress or eliminate this effect, as illustrated in Figure 2b. Furthermore, in marine seismic acquisition, the qSV mode is typically not recorded because hydrophones are placed in an isotropic water layer where this wave does not propagate. For this reason, we adopted this approach in the Marmousi model: the seismic source is located in an isotropic region and the wavefield subsequently propagates into an anisotropic medium. However, it may represent a significant limitation in land seismic surveys, where the qSV component can be relevant.

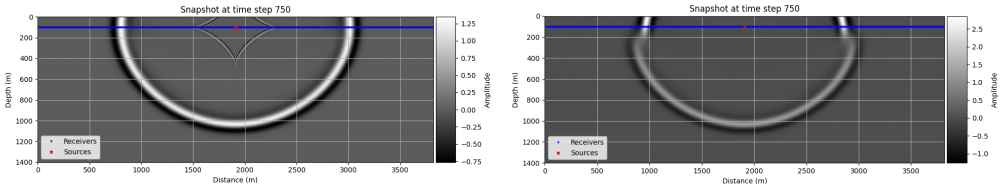

(a) (b)

Figure 2: Snapshot of the wavefield with $\epsilon = 0.2$ and $\delta = 0.1$. (a) Homogeneous anisotropic medium. (b) Two-layer model: isotropic upper layer and anisotropic lower layer. The wavefields are shown at time $t = 0.375$ s.

After validation, the Marmousi model (Figure 3a), widely used as a benchmark in seismic modeling due to its geological complexity, was adopted as the main scenario for comparison between acoustic and VTI pseudo-acoustic models. Seismograms were generated for both models (acoustic and VTI pseudo-acoustic), and the residual between them was computed to quantify their differences.

The models have dimensions of 3820 m (horizontal) and 1400 m (depth), discretized on a regular grid with spacing $\Delta x = \Delta z = h = 10$ m and a time step of $\Delta t = 0.0005$ s. The seismic source was placed at coordinates [x, z] = [1910 m, 100 m], with a cutoff frequency of 60 Hz. To generate the density, epsilon, and delta models from the Marmousi P-velocity model, we followed the Gardner relation as referenced by Rosa (2010) to estimate the density, along with the methodology proposed by Petrov et al. (2021) to obtain the anisotropic parameters:

$$\rho = aV_p^b\ , \qquad \epsilon = 0.25\rho - 0.3 \qquad \text{and} \qquad \delta = 0.125\rho - 0.1, \tag{5}$$

Where ρ is the density of the medium, and $a = 0.23$, $b = 0.25$ are empirical constants.

Results

In the acoustic model (Figures 3b), wavefronts are nearly circular, reflecting isotropic propagation behavior. In contrast, the VTI model (Figure 3c) shows wavefronts elongated in horizontal direction, indicating that propagation velocity varies with direction. This behavior demonstrates the significant role of anisotropy, especially in geologically complex media, where it cannot be ignored. Thus, considering VTI anisotropy is essential for more accurate seismic modeling and imaging.

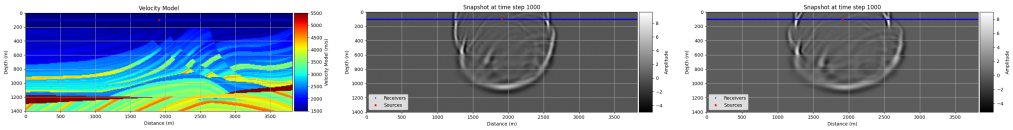

(a) (b) (c)

Figure 3: (a) Marmousi velocity model. (b) Snapshot of acoustic wave propagation in the model. (c) Snapshot of pseudo-acoustic VTI wave propagation in the model. The figures show the wavefields at time t = 0.5 s.

A comparison of the seismograms (Figure 4c) further supports these observations. The first arrivals are nearly identical in both models (Figures 4a and 4b), which is expected, since the water layer is isotropic and the velocity contrasts in shallow sediments are minimal. However, at greater depths and larger offsets, noticeable differences appear in arrival times, waveforms, and amplitudes. These differences arise from anisotropy, which affects wave propagation, especially in the horizontal direction, due to parameters ϵ and δ that influence phase velocity.

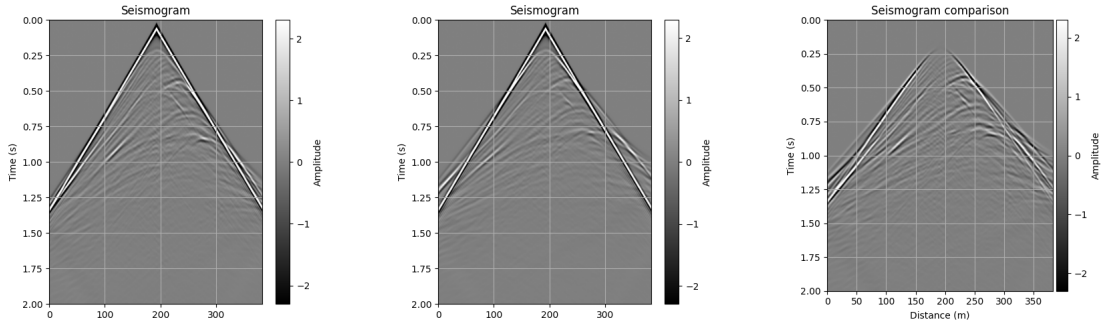

(a) (b) (c)

Figure 4: Seismograms generated for the Marmousi model using (a) the acoustic model, (b) the pseudo-acoustic VTI model, and (c) the residual between them.

Conclusions

In summary, the comparison between acoustic and VTI models in the Marmousi scenario shows that anisotropy significantly affects seismic wave propagation, especially at greater depths and larger offsets. Including anisotropic effects provides a more accurate representation of the complexity of real media, improving the fidelity of simulated seismic responses. Therefore, for applications requiring high-precision modeling VTI models are essential. As the next step in this research, we intend to investigate how anisotropy influences seismic imaging through Reverse Time Migration (RTM).

References

Alkhalifah, T., 1998, An acoustic wave equation for anisotropic media: SEG Technical Program Expanded Abstracts 1998, Society of Exploration Geophysicists, 1913–1916.

Cerjan, C., D. Kosloff, R. Kosloff, and M. Reshef, 1985, A nonreflecting boundary condition for discrete acoustic and elastic wave equations: Geophysics, **50**, 705–708.

McGarry, R., and P. Moghaddam, 2009, NPML boundary conditions for second-order wave equations: SEG Technical Program Expanded Abstracts, **28**, 3590–3594.

Petrov, I. B., V. I. Golubev, V. Y. Petrukhin, and I. S. Nikitin, 2021, Simulation of Seismic Waves in Anisotropic Media: Doklady Mathematics, **103**, 146–150.

Rosa, A. R. L. R., 2010, Análise do Sinal Sísmico.

Tsvankin, I., 1997, Anisotropic parameters and P -wave velocity for orthorhombic media: GEOPHYSICS, **62**, 1292–1309.

Acknowledgments

The authors from Fluminense Federal University acknowledge the financial support from Petrobras through the R&D project *Modelagem Visco-Elástica Anisotrópica em dados Multi-Azimutais para Análise de Sensibilidade de Sistemas de Fraturas* (ANP nº 24643-9). The strategic importance of the R&D levy regulation of the National Agency for Petroleum, Natural Gas and Biofuels (ANP) is gratefully appreciated.